Transitions of macroscopic structures and self-induced chaos observed in plasmas by a dc hollow cathode discharge having features of nonlinear open systems

Y. Kondoh, T. Ubusawa, D. Asanuma, Y. Hayakawa, A. Matsuoka, and T. Takahashi
Department of Electronic Engineering, Gunma University, Kiryu, Gunma 376-8515, Japan

M. Goto
Department of Electronic Engineering, Hokuriku Polytechnic College, Uozu, Toyama 937-0856, Japan

T. Okada
Department of Information Engineering, Maebashi Institute of Technology, Maebashi, Gunma 371-0816, Japan

A novel experimental investigation is presented on the connection between discontinuous transitions of macroscopic structures of plasma and self-induced chaotic oscillations characterized by the positive Lyapunov exponents λ_L through the period-doubling route in a dc hollow cathode discharge, which has features of nonlinear open systems. We have clarified experimentally that there appear different discharge modes accompanying the discontinuous transitions, and detailed qualitative explanations are presented about the mechanism of those transitions. It is shown that fundamental frequencies of the self-induced periodic oscillations with nonpositive λ_L change with the changes of discharge current, and the amplitude of chaotic oscillations with the positive λ_L jumps up almost one order higher than that of nonchaotic ones with the nonpositive λ_L. The self-induced chaotic oscillations with the positive λ_L have been observed near two edges of discontinuous transitions of plasma structures, suggesting that the chaotic mode is associated with the discontinuous transition of macroscopic structures in some nonlinear open systems.

PACS number(s): 52.35.Ra, 05.45.−a, 52.80.−s

I. INTRODUCTION

The subject of order and chaos in dissipative nonlinear systems has been extensively studied in many fields such as in physics, chemistry, and biology [1]. In the case of physics, many experimental studies on chaos have been performed in nonlinear systems such as nonlinear circuits [2] or gaseous lasers [3]. The gaseous plasma in glow discharges is one of such interesting nonlinear systems, where the externally driven chaos [4,5] and the self-induced one [6,7] through Feigenbaum's period-doubling route [8] have been experimentally observed. Cylindrical hollow-cathode discharges are also known to exhibit the self-induced oscillations and the chaotic behavior [9–11]. The mechanism, which increases plasma density dramatically in the hollow cathode discharge compared with use of the usual anode–cathode discharge, has not been clarified enough experimentally and theoretically yet. The self-induced chaos has been found recently in peripheral plasmas of a fusion device [12]. A theoretical investigation of externally driven chaos in plasmas has been reported in the work [13] showing that an ion fluid model in the sheath potential with a low degree of freedom (three variables) agrees fairly well with experimental results of the period-doubling route to chaos in the special plasma device of the double layer system [14,15]. Experimental observations of chaos in the gaseous plasma reported hitherto, however, have not been connected with macroscopic structures of plasma itself, even though the observations have revealed the property of the low dimensional deterministic chaos [4–7,9–13]. Since the gaseous plasma is a typical nonlinear dynamical ''open system'' with a large number of degrees of freedom, especially in the case of the hollow cath-

ode discharge, the chaotic behavior of plasma is considered to have strong connections with the macroscopic structures of plasma. In this paper we report a novel experimental investigation on the connection between the macroscopic structures of plasma, self-induced periodic oscillations, and the self-induced chaos through the period-doubling route and also the intermittent one in a dc hollow cathode discharge. Experimental results show that the self-induced chaos, characterized by the positive Lyapunov exponents, relates with discontinuous mode transitions of the macroscopic structures of plasma produced in the hollow cathode.

II. EXPERIMENTAL METHODS

The experimental apparatus used for the dc hollow cathode discharge is schematically shown in Fig. 1, where the top cross-sectional view of the chamber, the figure of the hollow cathode, and the side cross-sectional view of the chamber with the discharge circuit are presented. The chamber and the anode, made of stainless steel, are connected to the earth. The hollow cathode is made of two parallel Al plates that are insulated from the chamber. The interval D of the two cathode planes is variable. Fixed sizes of the used apparatus are shown in each figure of Fig. 1. The chamber is evacuated to a base pressure of about 1.0×10^{-3} Torr and filled with argon as a working gas. The working Ar pressure (P_a) is set by a flow gauge valve, and therefore the discharge plasma is surrounded by this background Ar gas with a little flow as an unfixed open boundary. The discharge is controlled by the Ar pressure P_a, the discharge voltage (V_d) between the anode and the hollow cathode, and the interval D of the cathode planes. The main diagnostic apparatus in-
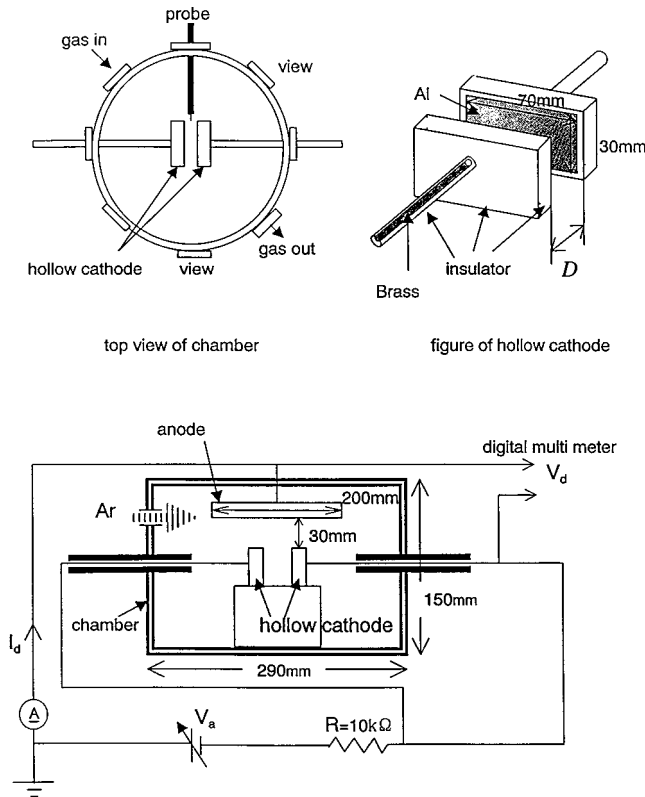
FIG. 1. Schematic figures of experimental apparatuses.

FIG. 2. Six basic structures of plasma for A- to F-modes, taken by the side view visible light.

volves movable double probes, a video recorder to observe time evolutions of visible plasma structures during increase or decrease of V_d, and a digital camera for visible light to analyze the macroscopic structures of plasma by computers. Here, one of the two cylindrical probes at the top of the double probes is used as a single Langmuir probe to measure the floating potential in the produced plasma. The measured data of the floating potential are recorded as digital data through an analog-to-digital transformer, and the digitized data are used to get the phase trajectories, the power spectra, and the Lyapunov exponents λ_L. A $x-y$ recorder is also used for the probe measurement, and for observations of discontinuous transitions on the characteristic curves with respect to the relations between the discharge current (I_d) and V_d. Using the method introduced by Sato, Sano and Sawada in [16], we calculated the maximum λ_L by the following equation,

$$\lambda_L = \frac{1}{\tau}\left\{ \frac{1}{N} \sum_{i=1}^{N} \ln\frac{|\mathbf{x}_i(t+\tau) - \mathbf{y}_i(t+\tau)|}{|\mathbf{x}_i(t) - \mathbf{y}_i(t)|} \right\}, \qquad (1)$$

where the pair of $\mathbf{x}_i(t)$ and $\mathbf{y}_i(t)$ denote possible near two points on the two trajectories in the phase space, N is the large number of sampling data points on the trajectories and τ is the sampling time.

III. EXPERIMENTAL RESULTS AND DISCUSSION

Changing experimental values of the set of (P_a, V_d, D), we have obtained six basic modes of discharge, called here
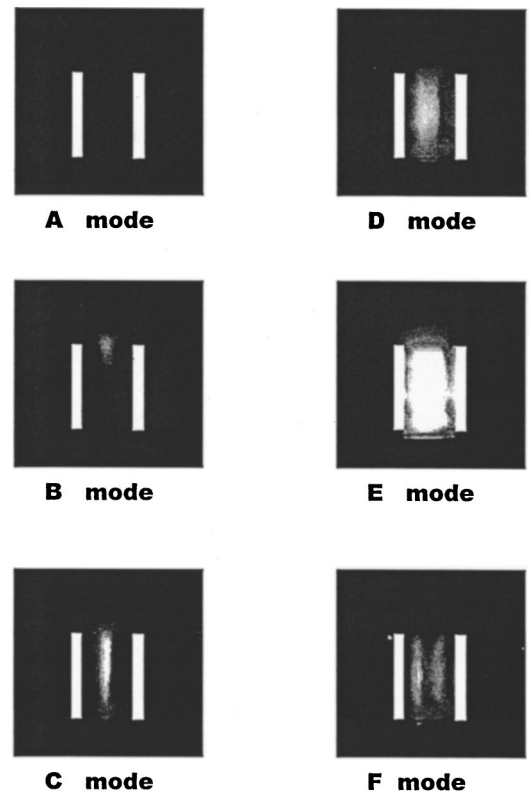
''A- to F-modes,'' whose typical macroscopic structures of plasma taken by the side view visible light inside the hollow cathode are shown in Fig. 2. In each figure, two parallel white blocks mark the hollow cathode, but the anode above the cathode is not shown. In the lower pressure region around 0.3 Torr, as the value of V_d is increased, the discharge mode sequentially changes from A- to E-modes, where the A-mode is the dark current region with little visible light. During the changes, there occur discontinuous sudden transitions of modes between A- to B-, B- to C-, and C- to D-modes, and there follows continuous transition from D- to E-modes. Here, the E-mode is distinguished from the D-mode by the different power dependence of I_d on V_d and the different luminous feature with the highest light intensity from plasmas. Here, in the two discontinuous transitions from B- to C- and C- to D-modes, using the video recorder, we have observed discontinuous sudden changes of luminous shape and thickness of plasma, which occur simultaneously with discontinuous transitions of $I_d - V_d$ characteristic curves traced by the $x-y$ recorder. In the higher pressure region more than 0.5 Torr, however, a direct discontinuous transition from A- to F-modes takes place, where the F-mode is characterized by the Faraday dark space at the center region of the hollow cathode. Those clear discontinuous transitions of macroscopic plasma structures between A- and B-, B- and C-, C- and D-, and A- and F-modes have not been reported yet, as far as the authors know. When we say simply ''the hollow cathode discharge,'' we should have to notice and refer to the fact that the discharge has the fine structures of

B-, C-, D-, E-, and F-modes. We can observe hysteresis on the I_d–V_d characteristic curves around each discontinuous transition of modes mentioned above.

From repeating careful observations with the use of the diagnostic apparatus, we present here the following qualitative explanations for the mechanism of each transition of modes that occur in the nonlinear open systems of the hollow cathode discharges under experimental conditions with various values of P_a and D.

(1) Discontinuous transition from A- to B-modes: As V_d increases, electrons composing the dark current are accelerated enough by the externally applied electric field, so that they ionize neutral particles to increase plasma densities. When the initially quite low plasma densities have reached some higher ones, the virtual anode is considered to be produced within a short time, extending near the upper area of the two plane cathodes. This is because the conductivity of the plasma between the anode and the two plane cathodes would increase as the plasma densities increase. The mechanism of this nonlinear mode transition, however, has not been clarified yet experimentally and theoretically and that is also one of the research objects attracting the present authors. The light shape of the B-mode plasma may be the result by the glow discharge between the virtual anode and the upper area of the two plane cathodes.

(2) Discontinuous transition from B- to C-modes: As V_d increases further, the produced plasma in the B-mode would diffuse around and also into the center area of the plane hollow cathode. When the plasma densities, diffused into the plane hollow cathode, have reached some higher ones, the virtual anode would extend more widely within a short time inside the plane hollow cathode, in the same way as the nonlinear mode transition from A- to B-modes, as mentioned above. The light shape of the C-mode plasma may be due to the glow discharge between the central virtual anode and the two plane cathodes. Within the C-mode region, the depth of the light shape grows deeper and deeper down to the bottom of the plane hollow cathode, as V_d increases.

(3) Discontinuous transition from C- to D-modes: As V_d increases further, the plasma densities around the midplane in the plane hollow cathode would increase higher and higher, just like the state shift from the normal to the abnormal glow discharge in the usual anode and cathode discharge, where the peak point of the plasma densities moves nearer to the cathode surface. The mechanism of the discontinuous transition process from C- to D-modes may be explained by the following more detailed model: (We consider the key mechanism for the discontinuous transition from C- to D-modes the same as that of the nonlinear transition from the α regime to the γ one in the capacitive coupled rf discharges, which we have investigated by computer simulations, as will be published elsewhere. In the case of the rf discharge, the changes of time averaged plasma densities and ion sheath widths are used in the detailed model.)

(3-A) As the plasma densities gradually increase higher and higher because of the higher ionization rate accompanied by the higher value of V_d, the widths of both ion sheaths, which cover the electrode surfaces of the plane hollow cathode, become narrower and narrower by the shielding effect of electrons.

(3-B) As the width of each ion sheath becomes narrower, the intensity of the electric field in the ion sheath grows greater and also the higher edge of ion densities reaches closer to each electrode surface.

(3-C) The resultant greater electric field in the ion sheath greatly accelerates the ions themselves towards each cathode surface, so that the accelerated ions bombard the cathode surface to emit the secondary electrons through the process of the so-called γ effect by ions, which we call here ''the first γ effect.''

(3-D) The emitted electrons by the first γ effect are accelerated more effectively by the greater electric field in the sheath, and the accelerated electrons ionize the background neutral gas to increase more both densities of electrons and ions through the avalanche of ionization inside the sheath region.

(3-E) The increased densities of electrons and ions again make the width of the ion sheath narrower, and the processes from (3-B) to (3-D) go on circulating as a positive feedback system with respect to the increment of the ion density near each surface of the plane hollow cathode.

(3-F) The circulatory nonlinear processes from (3-B) to (3-E) continue to saturate to lead to the D-mode until establishment of the balance between productions and losses of ions in the sheath region, where the former is due to the ionization, and the latter is due to diffusions towards surrounding regions of the central bulk plasma, the electrodes, and the chamber.

(3-G) Since the circulatory nonlinear processes from (3-B) to (3-F) are the positive feedback ones, the transient time from C- to D-modes would be very short, referred as the discontinuous transition here, in the time scale of the present observations by the video and the $x-y$ recorders, as will be shown later. The first γ effect by ions may be dominant in the transition from C- to D-modes, compared with that by photons, which we call here ''the second γ effect,'' radiated from excited neutrals due to excitation collisions by electrons in the discharge region.

(4) Continuous transition from D- to E-modes: As V_d increases further within the D-mode, the discharge current densities and the electron ones go up more to affect excitation collisions that will result in higher intensity of light emission from the bulk plasma. This higher intensity of light emission would lead to the increase of secondary electrons through the process of the second γ effect by photons. This second γ effect may become gradually and relatively dominant to lead to E-mode, which has the different power dependence of I_d on V_d and the different luminous feature with the highest light intensity from plasmas, compared with the D-mode as mentioned at Fig. 2.

We have obtained experimental data shown below by decreasing the value of V_d from high values, because of easier setting of V_d. We have observed the self-induced chaos through the period-doubling route associated with the two discontinuous transitions of the macroscopic structures of plasma from D- to C- and from C- to B-modes, as will be
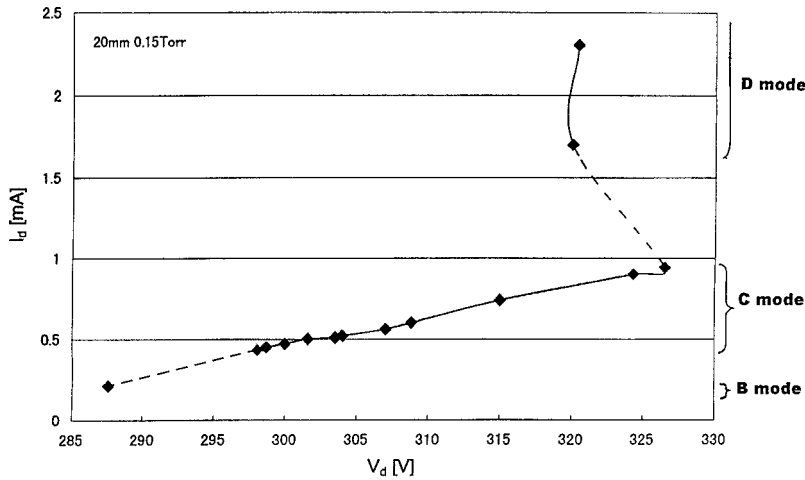
FIG. 3. Typical $I_d - V_d$ characteristic curve. $P_a = 0.15$ Torr. $D = 20$ mm. Broken lines denote transitional regions of discontinuous mode transitions.

shown below. Typical plasma parameters of the electron density n_e and the electron temperature T_e measured by the double probes at the midplane in the hollow cathode are as follows for the case of $D = 10$ mm and $P_a = 0.34$ Torr: For the C-mode discharge with $I_d = 5$ mA and $V_d = 348$ V, $n_e = 0.67 \times 10^{10}$ cm^{-3} and $T_e = 4.33$ eV. For the D-mode discharge with $I_d = 18$ mA and $V_d = 322$ V, $n_e = 1.23 \times 10^{10}$ cm^{-3} and $T_e = 4.54$ eV. For the E-mode discharge with $I_d = 30$ mA and $V_d = 330$ V, $n_e = 3.59 \times 10^{10}$ cm^{-3} and $T_e = 3.71$ eV.

Figure 3 shows a typical $I_d - V_d$ characteristic curve measured for a case with $P_a = 0.15$ Torr and $D = 20$ mm. Here, marks on the curve represent the data points for which we have gotten power spectra, phase trajectories, and the Lyapunov exponents λ_L from the data of the fluctuating floating potential V_f measured at the boundary plasma inside the hollow cathode. The discontinuous transition of the macroscopic structures of plasma mentioned in Fig. 2 occurs at two transitional regions shown by broken lines between two regions of B- and C-modes and C- and D-modes marked on the right-hand scale of Fig. 3. Negative differential resistance appears at the transitional region between C- and D-modes, associated with the discontinuous transition of a plasma structure. As was mentioned in Fig. 2, we observe hysteresis on the $I_d - V_d$ characteristic curves around each discontinuous transition of modes. We cannot settle the point at any aimed position on the discontinuous region of the $I_d - V_d$ curve in the present plane hollow cathode discharge, not like the usual $I - V$ curve of the simple plane anode–cathode discharge. This is because the discontinuous transition of the $I_d - V_d$ curve is not controllable due to nonlinear sudden transition of the macroscopic plasma structure in the hollow cathode, whose transition mechanism is yet unsolved. At present, we cannot draw the load line on the $I_d - V_d$ curve used for the present simple plane hollow cathode discharge. We have to leave the detailed investigation on the hysteresis in the $I_d - V_d$ characteristic curve in the case of the hollow cathode discharge to our future works.

In Fig. 4 we show a typical set of data (the temporal evolution of the floating potential V_f, the trajectory in phase space of V_f and dV_f/dt, and the power spectra), which were measured at the neighboring three points of marks on the $I_d - V_d$ curve around the transitional region between C- and D-modes shown in Fig. 3. Here, Figs. 4(a) and 4(b) show, respectively, the data at $V_d = 324$ V with $\lambda_L = -95.4$ and 326 V with $\lambda_L = -23.6$ within the C-mode region, and Fig. 4(c) shows the data at $V_d = 320$ V with $\lambda_L = 408$ within the D-mode region. The wave form, the trajectory with the negative λ_L, and the power spectra in Fig. 4(a) represent the self-induced periodic oscillation of V_f with a frequency f about 6.45 kHz and its harmonics. This fairly low frequency f suggests that the observed oscillation comes from the macroscopic motions of the ion fluid composed with heavy mass of Ar. When V_d is increased a little from 324 to 326 V, the value of λ_L is kept negative and a very clear period-doubling is observed as shown in Fig. 4(b) in the C-mode region. Then, there occurs discontinuous transition from C- to D-modes with the jump of V_d down to 320 V, and the wave form and the trajectory turn into a chaotic mode having the features with the positive λ_L and the continuous power spectra, as shown in Fig. 4(c). (In this experiment, real time sequences of measurements were from Fig. 4(c) to Fig. 4(a), as mentioned in Fig. 2.) It is emphasized here that the amplitude of fluctuation of the floating potential V_f jumps up to one order higher values in Fig. 4(c) of the chaotic mode with the positive λ_L than the cases of Figs. 4(a) and 4(b) with the negative λ_L. It is seen from Figs. 3 and 4 that there exists a period-doubling sequence to chaos which is accompanied by the discontinuous transition of the discharge mode, i.e., a discontinuous change of the macroscopic structure of plasma, in the dc hollow cathode discharges.

The phenomenon that the amplitude of V_f jumps up to one order higher values in Fig. 4(c) of the chaotic mode in the D-mode than the cases of Figs. 4(a) and 4(b) in the C-mode can be explained as follows: The plasma density in the case of Fig. 4(c) of the D-mode increases almost twice that in the case of Fig. 4(b) of the C-mode, as is known by data using the double probe measurement. The ion sheath width also decreases extremely from the case of Fig. 4(b) of the C-mode to that of Fig. 4(c) of the D-mode, and therefore the electrical field that accelerates electrons increases relatively very large in the ion sheath of the D-mode. The V_f
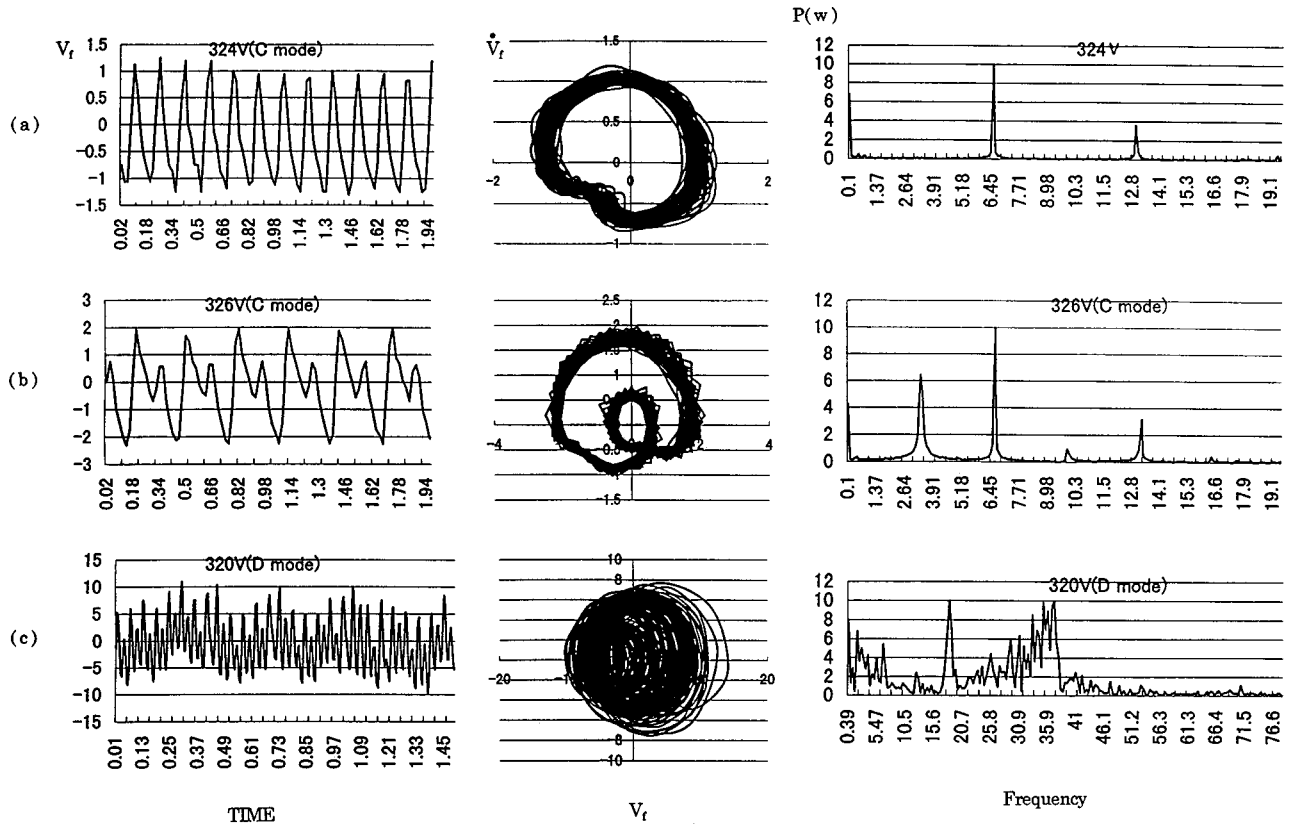
FIG. 4. A period-doubling sequence to chaos observed around the transitional region between C- and D-modes shown in Fig. 3. Scales of time, V_f, dV_f/dt, and frequency are ms, mV, mV/s, and kHz, respectively. (a) $V_d = 324$ V within the C-mode. $\lambda_L = -95.4$. (b) $V_d = 326$ V within the C-mode. $\lambda_L = -23.6$. (c) $V_d = 320$ V within the D-mode. $\lambda_L = 408$.

signal, which is measured by the single probe, results from mainly the density and energy of electrons surrounding the probe. The chaotic V_f fluctuations therefore increase fairly high through the discontinuous transition from Fig. 4(b) of the C-mode to Fig. 4(c) of the D-mode with the higher plasma density and with the extremely thinner ion sheath width.

We can recognize that the power spectrum in Fig. 4(c) in the case of the D-mode appears to have some coherent peaks. These coherent peaks can be explained as follows: The data of Fig. 4(c) has the positive value of Lyapunov exponents $\lambda_L = 408$, and the power spectrum of the data appears to have a coherent peak at about 18.2 kHz and possibly another at 36.4 kHz. These coherent peaks may be explained qualitatively as follows: Since these coherent frequencies are low, the fluctuation signal may be due to motions concerned with the ion mass. The bulk plasma within the two plane hollow cathode may naturally have various types of macroscopic oscillations such as moving back and forth between the two cathodes, changing the thickness and the height of the bulk plasma region itself, and so on. The single probe signal carries energies of electrons, which are passing through the two ion sheath regions of the plane hollow cathode and also through the bulk plasma having the two or more coherent oscillations mentioned above. Because these mechanisms, the single probe signal should be the mixture of the coherent and the chaotic oscillations.

When we decrease values of V_d in the C-mode region towards the transitional region with the B-mode one, the self-induced oscillations of V_f with the frequency f bifurcate into the state of $f/2$ and sometimes into the state of $f/3$, all of which have nonpositive λ_L. After those bifurcations of the self-induced oscillations, we can observe again the chaotic mode of oscillations with the positive λ_L within the C-mode region near the transitional region. The amplitude of the fluctuation of V_f of the chaotic mode also jumps up almost one order higher in this case, in the similar way as shown in Fig. 4.

Keeping V_d to be 324 V without changing all other experimental conditions, we obtain a series of data of V_f along the time within a few minutes, as shown Fig. 5, where Fig. 5(a) shows the same data as Fig. 4(b). Comparisons among the data of Fig. 5(a) ($\lambda_L = -95.4$), 5(b), and 5(c) ($\lambda_L \simeq 90.0$) clearly show us that the period doubling takes place and leads to the chaotic oscillations along the time within a few minutes, i.e., intermittent chaos. In the case of intermittent chaos, the amplitude of fluctuation of V_f does not have significant jumps, unlike in Fig. 4. This is because the discharge mode stays in the same C-mode without occurrence of the discontinuous mode transition. This type of intermittent chaos will be shown more clearly in the next figure.

We have calculated the values of the Lyapunov exponents λ_L for all data points marked on the $I_d - V_d$ characteristic
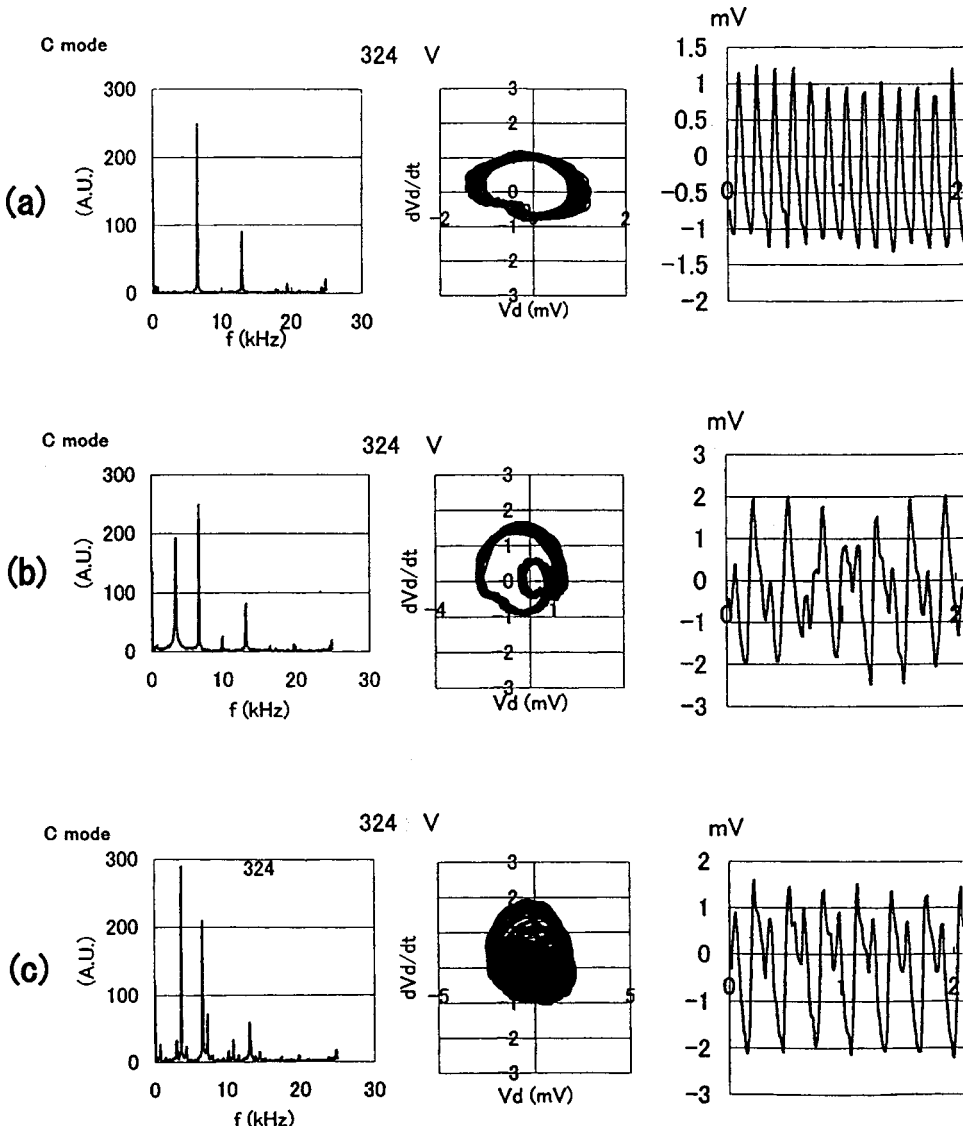
FIG. 5. A series of the intermittent chaos along the time within a few minutes, keeping the value of V_d to be 324 V in the C-mode. Scales of time, V_f, dV_f/dt, and frequency are ms, mV, mV/s, and kHz, respectively. (a) $\lambda_L = -95.4$. (b) λ_L is not calculated. (c) $\lambda_L \simeq 90.0$.

curve in Fig. 3. The resultant dependence of λ_L values on the discharge current I_d is shown in Fig. 6, where the mark ○ at $I_d \simeq 0.2$ mA represents that data of the V_f noise level. In the figure, there are two jump regions of I_d, where the lines connecting neighboring data points are shown by dashed lines, corresponding to the two transitional regions between B- and C-modes and C- and D-modes. The chaotic modes of oscillations mentioned above are observed at the data points with positive values of λ_L near the edges of the two transitional regions of discharge modes. At $I_d \simeq 0.9$ mA, where $V_d = 324$ V, we see two close data points, one of which has a negative value of λ_L and the other a positive one. These two data points represent the intermittent chaos mentioned in Fig. 4.

The frequency f of the self-induced oscillations of V_f shifts as the discharge parameter V_d or I_d changes. The dependence of the frequency f, determined from the power spectra, on the discharge current I_d is shown in Fig. 7 for the same marked data in Fig. 3. Here the mark ○ at $I_d \simeq 0.2$ mA represents that data of the V_f noise level. In Fig. 7, there are also two jump regions of I_d without data points,

corresponding to the two transitional regions between B- and C-modes and C- and D-modes. The clear chaotic modes of oscillations mentioned above are observed at $I_d \simeq 1.7$ mA (the lower edge of the D-mode) and at $I_d \simeq 0.43$ mA (the lower edge of the C-mode), and only dominant frequencies are plotted in the figure for the clear chaotic cases. Near the edge of the D-mode region, the self-induced chaotic oscillations have relatively higher and continuous frequencies, as was shown in Fig. 4(c). As I_d is decreased in the C-mode region, fundamental frequency slightly increases at first (from the upper edge of the C-mode region to the point with $I_d \simeq 0.6$ mA), and the period-doubling bifurcations take place during the increase of f. In this region of I_d, luminous thickness of plasma becomes thinner and thinner as I_d decreases, but the depth of plasma is kept from the top to the bottom in the hollow cathode. The self-induced oscillations of V_f, however, become to be almost undetectable at $I_d \simeq 0.55$ mA. After this point, as I_d decreases to the lower edge of the C-mode region, fundamental frequency decreases accompanied by bifurcations of $f/2$ or $f/3$ states, and the depth of the plasma becomes shorter and shorter to almost
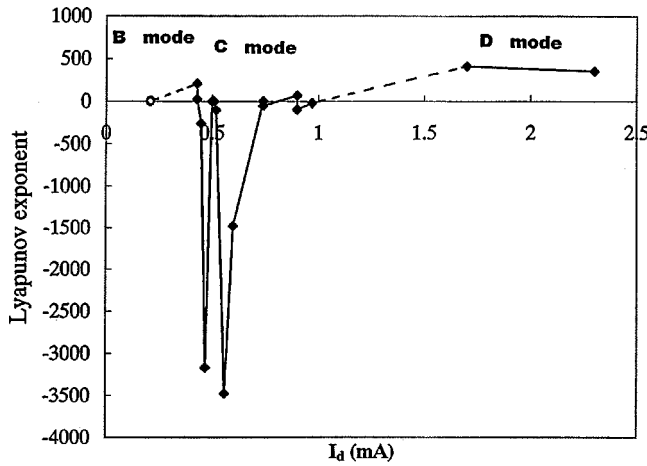
FIG. 6. Dependence of the Lyapunov exponents λ_L on the discharge current I_d obtained from the same marked data in Fig. 3. The mark ○ at $I_d \simeq 0.2$ mA represents that data of the V_f noise level.
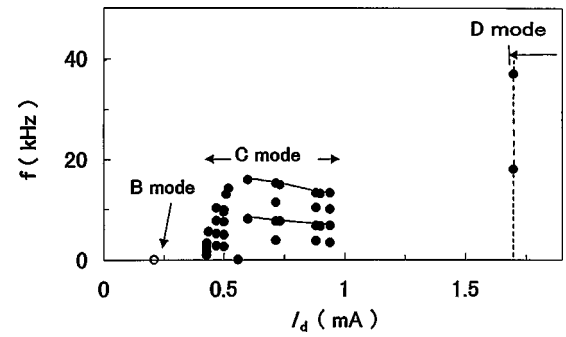

FIG. 7. Dependence of oscillation frequency f on the discharge current I_d obtained from the same marked data in Fig. 3. The mark ○ at $I_d \simeq 0.2$ mA represents that data of the V_f noise level.

half depth of the hollow cathode. Near the lower edge of the C-mode region at $I_d \simeq 0.43$ mA, the self-induced oscillations of V_f become chaotic again, having relatively lower and continuous frequencies, as is seen from Fig. 7.

We expect from the data shown in Figs. 5 and 6 that the following two experimental results of (a) and (b) belong to essential features of nonlinear open systems:

(a) The fundamental frequency of the self-induced oscillations gradually changes as the control parameter of I_d changes.

(b) The appearance of chaotic modes is strongly connected with the mode transitions of the macroscopic structures of plasma.

IV. CONCLUDING REMARKS

We have presented a novel experimental investigation on the connection between the discontinuous transitions of macroscopic structures of plasma and the self-induced chaotic oscillations in a dc hollow cathode discharge that has features of nonlinear open systems. We have clarified that there exist the fine structures of B-, C-, D-, E-, and F-modes in the dc hollow cathode discharge (cf. Fig. 2). The discontinuous transitions occur between A- and B-modes, B- and C-modes, and C- and D-modes. We can observe hysteresis on the $I_d - V_d$ characteristic curves around each discontinuous transition of these modes. From repeating careful observations using the diagnostic apparatus, we have presented the qualitative explanations from (1) to (4) for the mechanism of corresponding mode transitions. The common process of the mechanism of discontinuous transitions between both A- and B-modes and B- and C-modes may be attributed to the rapid extension of the virtual anode that occurs in the gaseous plasma. The dominant process in the discontinuous transition from C- to D-modes, however, may be explained by another circulating positive feedback process with respect to the increment of ion densities near the cathode surface due to the first γ effect by ion bonbardment at the cathode [cf. the

detailed explanations from (3-A) to (3-G) at the explanation (3)]. The continuous transition from D- to E-modes may be explained by the second γ effect by photons due to higher light radiation from the bulk plasma. This second γ effect gives gradual increment of the secondary electron emission that may increase excitation collisions, some part of which lead again to the second γ effect, giving rise to the E-mode specified by different power dependences of I_d on V_d and different luminous features with the highest light intensity from plasmas.

We have shown that there appear the self-induced chaotic modes of oscillations which are characterized by positive Lyapunov exponents λ_L through the clear period-doubling route (cf. Fig. 4). It should be emphasized here that the amplitude of the self-induced chaotic oscillations jumps up to almost one order higher than the periodic ones with nonpositive λ_L and the chaotic oscillations accompany the discontinuous mode transitions of the macroscopic structures of plasma, as was clearly demonstrated by two jump regions of discharge current and the positive values of λ_L shown in Fig. 6.

When we decrease values of V_d in the C-mode region towards the transitional region with the B-mode one, the self-induced oscillations of V_f with the frequence f bifurcate into the state of $f/2$ and sometimes into the state of $f/3$, all of which have nonpositive λ_L (cf. the C-mode region in Fig. 6).

Keeping the value of V_d, we have obtained two sets of data, one of which shows the periodic oscillations with nonpositive λ_L and the other the chaotic ones with the positive λ_L (cf. at $I_d \simeq 0.9$ mA in Fig. 6). This experimental result indicates that the intermittent chaos also appears in this dc hollow cathode discharge (cf. Figs. 5 and 6).

We have clarified that the fundamental frequency of the self-induced periodic oscillation changes with the value of I_d and it correlates closely with the macroscopic structures of plasma, such as the thickness and the size of luminous plasma inside the plane hollow cathode (cf. the C-mode region in Fig. 7).

We have observed an interesting phenomenon from the higher edge of the C-mode region, the luminous thickness of plasma becomes thinner and thinner as I_d decreases, and the self-induced oscillations of V_f suddenly reduce to almost undetectable amplitude at the point of $I_d \simeq 0.55$ mA and V_d

=307 V in Fig. 3, as was seen in Fig. 7. Both sides of this point, the self-induced periodic oscillations, can be observed clearly (cf. Fig. 7).

We may conclude from the present experimental results that the following two facts of (a) and (b) belong to essential features of nonlinear open systems, such as the hollow cathode discharge system.

(a) The fundamental frequency of the self-induced oscillations gradually changes as the control parameter of I_d changes.

(b) The discontinuous transitions of macroscopic structures of plasma take place with the appearance of the self-induced chaotic oscillations having large amplitude of fluctuations.

[1] *Evolution of Order and Chaos in Physics, Chemistry, and Biology*, edited by H. Haken, Springer Series in Synergetics Vol. 17 (Springer-Verlag, Berlin, 1982).
[2] P.S. Linsay, Phys. Rev. Lett. **47**, 1349 (1981).
[3] C.O. Weiss, A. Godone, and A. Olafsson, Phys. Rev. A **28**, 892 (1983).
[4] P.Y. Cheung and A.Y. Wong, Phys. Rev. Lett. **59**, 551 (1987).
[5] F. Greiner, Phys. Rev. Lett. **70**, 3071 (1993).
[6] T. Braun, J.A. Lisboa, and J.A.C. Gallas, Phys. Rev. Lett. **59**, 613 (1987).
[7] J. Qin, L. Wang, D.P. Yuan, P. Gao, and B.Z. Zhang, Phys. Rev. Lett. **63**, 163 (1989).
[8] M. J. Feigenbaum, J. Stat. Phys. **19**, 50 (1978).
[9] K. Tochigi, S. Maeda, and C. Hirose, Phys. Rev. Lett. **57**, 711 (1986).
[10] R. Singh, P.S.R. Prasad, J.K. Bhattacharjee, and R.K. Thareja, Phys. Lett. A **178**, 284 (1993).
[11] P.S.R. Prasad, R. Singh, and R.K. Thareja, IEEE Trans. Plasma Sci. **22**, 224 (1994).
[12] A. Komori, Phys. Rev. Lett. **73**, 660 (1994).
[13] M. Kono and A. Komori, Phys. Fluids B **4**, 3569 (1992).
[14] N. Ohno, A. Komori, M. Tanaka, and Y. Kawai, Phys. Fluids B **3**, 228 (1991).
[15] A. Komori, M. Kono, T. Norimine, and Y. Kawai, Phys. Fluids B **4**, 3573 (1992).
[16] S. Sato, M. Sano, and Y. Sawada, Prog. Theor. Phys. **77**, 1 (1987).